Low-temperature magnetic and transport properties of single-crystal CeCoGe

2008 J. Phys.: Condens. Matter 20 465223

(http://iopscience.iop.org/0953-8984/20/46/465223)

J. Phys.: Condens. Matter **20** (2008) 465223 (5pp) doi:10.1088/0953-8984/20/46/465223

Low-temperature magnetic and transport properties of single-crystal CeCoGe

M ElMassalami[1], R E Rapp[1], J P Sinnecker[1], A V Andreev[2] and J Prokleška[3]

[1] Instituto de Fisica, Universidade Federal do Rio de Janeiro, Caixa Postal 68528, 21945-970 Rio de Janeiro, Brazil
[2] Institute of Physics ASCR, Na Slovance 2, 18221 Prague 8, Czech Republic
[3] DCMP, Faculty of Mathematics and Physics, Charles University, Ke Karlovu 5, 12116 Prague 2, Czech Republic

Received 1 September 2008, in final form 26 September 2008
Published 27 October 2008
Online at stacks.iop.org/JPhysCM/20/465223

Abstract

The low-temperature properties of single-crystal CeCoGe were investigated by specific heat $C(T, H)$, magnetoresistivity $\rho(T, H)$, and differential susceptibility measurements $\chi(T, H)$. The zero-field low-temperature specific heat evolves as $C = \gamma T + \beta T^3 = 42T + 23.5T^3$ mJ mol^{-1} K^{-1}. On comparing its $\gamma = 42$ mJ mol^{-1} K^{-1} with that of LaCoGe (12 mJ mol^{-1} K^{-2}) it is inferred that both 3d (Co) and 4f (Ce) orbitals contribute to the density of states at the Fermi level. Assuming that its phonic contribution to the specific heat is similar to LaCoGe ($\beta = 0.5$ mJ mol^{-1} K^{-4}), then the extra cubic term in the specific heat ($23T^3$ mJ mol^{-1} K^{-1}) must be due to magnon excitation within the antiferromagnetically ordered state, $T < T_N$. On the other hand, the thermal evolution of the resistivity is found to be dominated by the following scattering processes: magnon scattering operating within the ordered state at $T < T_N$ leading to a T^4 resistive contribution and a spin fluctuation process associated with the Co subsystem giving rise to both a quadratic resistive term below 15 K and a saturated resistive term at higher temperatures. The isothermal magnetoresistivity below T_N, $\rho(T < T_N, H)$, manifests a peak which is centered at the same critical field that appears in the magnetization isotherms. This peak, together with the peak observed at a temperature 0.7 K below T_N, is attributed to a spin rearrangement of the AFM structure of the Ce sublattice.

(Some figures in this article are in colour only in the electronic version)

1. Introduction

The Ce 4f orbitals in Ce-based intermetallic compounds have the tendency to spatially extend over a region wider than their atomic size, and as such give rise to a variety of electronic effects such as delocalization, spin fluctuation, non-Fermi liquid behavior, etc. A similar spatial charge spread occurs frequently in Co-based intermetallics: the Co 3d orbitals have a tendency to form electronic bands. Depending on factors such as band filling and the local magnetic field at the Co site, this spread may give rise to a variety of magnetic states such as itinerant magnetism, spin fluctuation, enhanced Pauli paramagnetism, etc. It is then of interest to see which of these electronic states is manifested in those intermetallic compounds that contain both Ce and Co atoms. In that case, it is important to identify and distinguish between the contributions of the Ce and Co subsystems to, say, the magnetic and electronic properties. To carry out such an analysis, one usually investigates the physical properties of highly pure single crystals by employing experimental techniques (such as transport, thermal, or magnetic measurements) that are conducted at very low temperatures and under high magnetic fields. With these intentions in mind, we studied the low-temperature properties of CeCoGe single-crystal. Comparison with LaCoGe was found to be extremely useful for identifying the above-mentioned individual contributions.

CeCoGe crystallizes in the CeFeSi-type structure with space group $P4/nmm$ [1]. Its magnetic structure at 2 K consists of ferromagnetic Ce (001) planes ($\mu_{Ce} \parallel a \approx 0.4\ \mu_B$) that are stacked antiferromagnetically along the c axis [2]. The

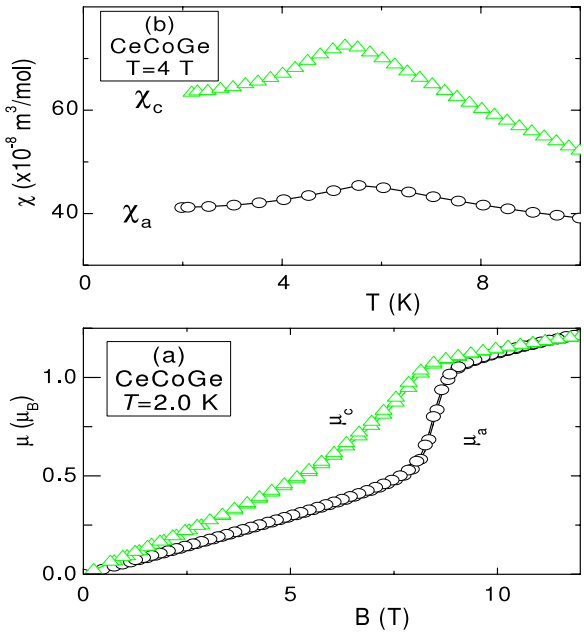

Figure 1. (a) Magnetization isotherms of CeCoGe measured at 2.0 K with the magnetic field applied along the a and c axes (see [4]). (b) The thermal evolution of the dc magnetic susceptibility of CeCoGe in a 4 T magnetic field applied along the a and c axes. It is noted that in such a field $T_N(H)$ and $T_M(H)$ approach each other (see the text).

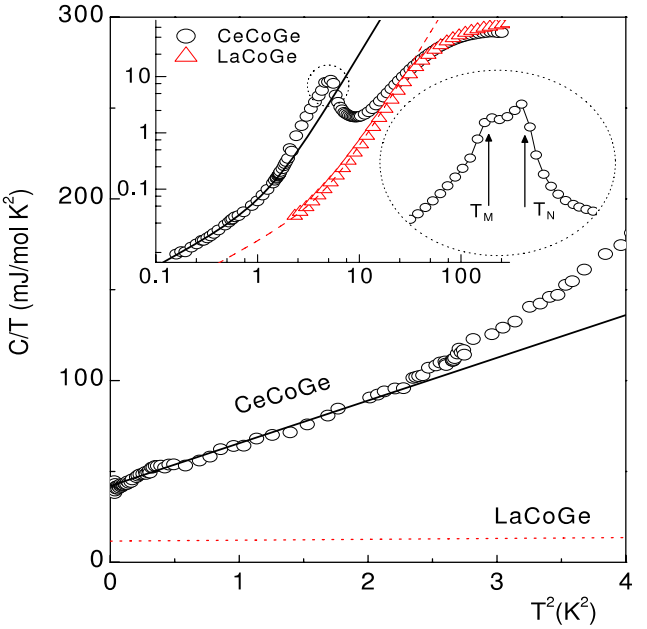

Figure 2. Zero-field C/T versus T^2 of CeCoGe (the extrapolation of LaCoGe is also included). The low-temperature part of CeCoGe is fitted to $C/T = 42 + 23.5T^2$ mJ mol^{-1} K^{-2} (solid line) while that of LaCoGe is given by $C/T = 12 + 0.5T^2$ mJ mol^{-1} K^{-2} (dotted line). The inset shows (on logarithmic scales and over three orders of magnitudes in temperature) the $C(T)$ curves of CeCoGe and LaCoGe. The specific heat data for $T > 2$ K are taken from [3]. Notice the two events at T_N and T_M.

magnetization curves [3, 4], on the other hand, reflect a strong anisotropy which extends to temperatures well above $T_N = 5.5$ K (the Curie–Weiss parameters [2–4] are $\mu_{eff} = 2.5\ \mu_B$, $\theta_p^{\|c} = -65$ K, $\theta_p^{\|a} = -25$ K). Field-induced metamagnetic transitions are evident in the magnetization isotherms of both poly- [2] and single-crystal [4] samples. Since both critical fields ($H_c^{\|c}$ and $H_c^{\|a}$, see figure 1(a)) decrease as T increases, it is inferred that these metamagnetic transitions are intrinsic to the Ce subsystem: if occurring in an itinerant Co subsystem, such metamagnetic transitions would hardly be temperature-dependent.

Furthermore, the magnetic properties of CeCoGe within the immediate neighborhood of T_N manifest two interesting features [3–5]: first, the specific heat curve (figure 2) reveals two neighboring peaks, one centered at T_N and the other at T_M, 0.7 K below T_N. An increase in the applied field induces a reduction in the height of both peaks as well as a downwards shift of their centers [3, 6]: the shift rate is faster for $T_N(H)$ than $T_M(H)$. On increasing the field above a certain H_c, the two peaks merge into a highly broadened, single peak (see figure 1(b)) that shifts to higher temperatures as H is increased. Secondly, the in-phase ac susceptibility component χ' shows a maximum at T_N [3]. On a further temperature decrease, the out-of-phase ac susceptibility component χ'' (a measure of the energy absorption) begins to increase monotonically below T_M.

In all the above-mentioned reports, the Co subsystem in CeCoGe matrix is depicted as being magnetically silent; thus magnetic correlations were assumed to be associated only with the Ce subsystem. Using low-temperature specific heat and magnetoresistivity techniques, this work shows that both 3d and 4f orbitals do contribute to the density of states at the Fermi level and that the electronic correlations within the Co subsystem are evident in both transport and specific heat results

2. Experiment

As we were interested in the identification and separation of the electronic, phonic, and magnon contributions to the measured physical properties, our investigation was extended down to 0.1 K range and carried out on single-crystal samples. The single-crystal plates (the wider surface is perpendicular to the c axis) were extracted from an ingot after being pulled out of a hot zone of a tri-arc furnace using a modified Czochralski method. Powder x-ray diffraction analysis confirmed that the samples are single-phase with the CeFeSi-type structure and with the expected lattice parameters [3, 4]. The zero-field specific heat $C(T)$ was measured on a semi-adiabatic set-up operating within the temperature range 0.1 K $< T <$ 3 K. The magnetoresistivity (employing the conventional four-point dc method) and the isothermal magnetization and dc susceptibility were measured using the field and temperature environment of a commercial Quantum Design equipment. While the specific heat measurement was intentionally restricted to the very low-temperature range, the latter techniques were utilized extensively within the neighborhood of T_N so as to investigate the above-mentioned two-peak features.

3. Results and discussion

3.1. Specific heat

The specific heat curve of CeCoGe is given in figure 2. For comparison, we also show the specific heat of the isomorphous LaCoGe (taken from Vejpravová *et al* [3]). Evidently the specific heats of both isomorphs are well described by $C/T = \gamma + \beta T^2$: for CeCoGe $C/T = 42 + 23.5T^2$ mJ mol^{-1} K^{-2}, while for LaCoGe $C/T = 12 + 0.5T^2$ mJ mol^{-1} K^{-2}. On comparing the γ values of these two isomorphs one infers that both 3d (Co) and 4f (Ce) orbitals contribute to the density of states at the Fermi level: on the one hand a comparison with LaCoGe shows that 29% of the involved electronic degrees of freedom are associated with the non-Ce subsystems while 71% are due to the Ce 4f subsystem; it is interesting to note that such a Ce sublattice contribution to the density of states is equal to that of the Ce sublattice in the orthorhombic TiNiSi-type CeNiGe (its $\gamma = 32$ mJ mol^{-1} K^{-2}) [7]; nevertheless the fact that these two compounds are not isomorphic does not allow us to draw direct conclusion from the equality of their Ce sublattice related $\gamma's$. It is recalled that the Ni subsystem in CeNiGe (in contrast to the Co subsystem in CeCoGe) is magnetically inactive.

LaCoGe and CeCoGe are expected to manifest equal Debye cubic terms (neglecting the small mass difference). For LaCoGe $\beta = 0.5$ mJ mol^{-1} K^{-4} (see figure 2), then the extra cubic contribution ($23T^3$ mJ mol^{-1} K^{-1}) must be due to the magnon contribution of the Ce sublattice AFM order. Classic spin wave theory [8] associates such a cubic term with a linear dispersion relation of magnon quasiparticles. In this theory, the cubic term is manifested for temperatures much higher than the energy gap. As the experimental data follow faithfully the cubic term down to 0.1 K (our lowest measured temperature), then the energy gap, if there is any, must be lower than this 0.1 K. This, in turn, suggests an extremely small anisotropic term: an unresolved contradiction when compared to the reported highly anisotropic Curie–Weiss temperatures [4]. According to this scenario, the low-temperature magnetization isotherms along different axes should not manifest strong anisotropy; rather if there is any it should not be higher than the one shown by the specific heat.

3.2. Resistivity

Based on the above inference that both 3d and 4f orbitals do contribute to the density of states at the Fermi level, it is expected that both charge carriers undergo inelastic scattering not only from conventional processes (such as electron–phonon and defect scattering leading, respectively, to a resistive contribution of ρ_{ep} and ρ_0) but also from two additional, dominant processes, namely the magnon and spin fluctuation scatterings. Scattering from magnon quasiparticles is dominant within $T < T_N$. Assuming a linear dispersion relation ($\omega \propto |k|$), then this scattering leads to $\rho_{mag} \propto T^4$ [9]. Scattering from a spin fluctuation process, on the other hand, is assumed to be dominated by electronic correlations within the 3d Co subsystem: such scattering should be manifested in those enhanced paramagnetic Co-based isomorphs even with

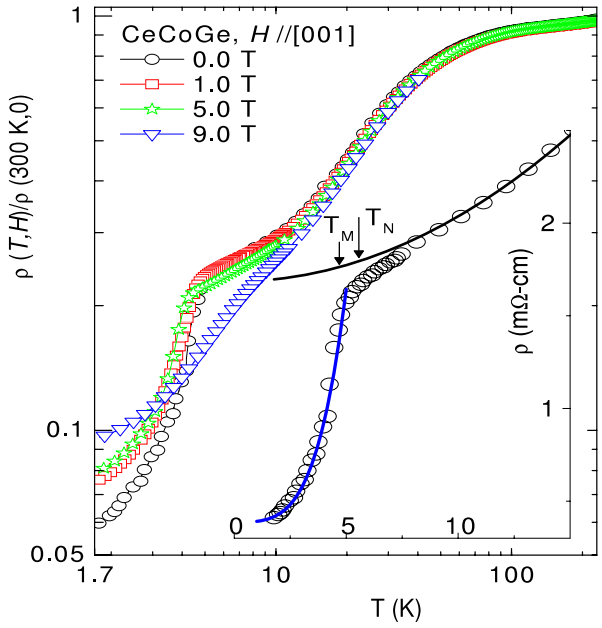

Figure 3. Log–log plot of the normalized resistivity $\rho(T, H)/\rho(300\text{ K}, 0\text{ T})$ of CeCoGe at representative magnetic fields. Inset: (symbols) the zero-field normalized resistivity on a linear and expanded scale. The fit for $T > T_N$ (solid line in the inset) describes $\rho_{tot}(T_N < T < 15\text{ K}) = 3.85 \times 10^{-6}T^2 + 16.9 \times 10^{-4}$ Ω cm, while the one for $T < T_N$ expresses $\rho_{tot}(T < T_N) = 3.85 \times 10^{-6}T^2 + 1.9 \times 10^{-4}T^4 + 3.9 \times 10^{-4}$ Ω cm (see the text). The short vertical arrows denote T_M and T_N as obtained from the specific heat.

nonmagnetic rare earth atoms, e.g. LaCoGe. This process gives rise to $\rho_{sf} \propto T^2$ at lower temperatures and a saturated resistivity at higher temperatures [10, 11].

The total resistivity reflects the combined influence of all these scattering processes, giving, if connection in series is assumed: $\rho = \rho_{ep} + \rho_0 + \rho_{mag} + \rho_{sf}$. Experimentally the thermal evolution of ρ is observed to be manifested as follows (see figure 3): first the high-temperature ($T > 100$ K) resistivity has a large and almost saturated value, typical of Co-based spin-fluctuating intermetallics such as the Laves-type phases RCo_2 (R = Lu, La) [12].

Secondly, on lowering the temperature below 100 K, $\rho(T, H)$ decreases very fast such that the ratio $\rho(6\text{ K})/\rho(300\text{ K}) \approx 0.2$ (see figure 3 and [2]). Such a drop, often observed in Co-based intermetallics, is usually attributed to a reduction in the spin fluctuation scattering [11, 12] (though relatively weak, Ce-related crystalline electric field (CEF) effects [13] may also be involved). In fact the inset of figure 3 does show the expected quadratic-in-temperature term of the spin fluctuation process: $\rho(T_N < T < 15\text{ K}) = AT^2 + \rho_0 = 3.85 \times 10^{-6}T^2 + 16.9 \times 10^{-4}$ Ω cm, where the constant ρ_0 expresses the Matthiessen sum of scatterings from defect centers (3.9×10^{-4} Ω cm) and Ce paramagnetic moments (13.0×10^{-4} Ω cm). The calculated ratio $A_{sf}/\gamma^2 \approx 2.18 \times 10^{-3}$ μΩ cm (mole K/mJ)$^{-2}$ is two orders of magnitude higher than the Kadowaki–Wood ratio [14], most probably because both γ and A are not solely due to one subsystem.

Thirdly, the resistive contribution due to scattering from magnon quasiparticles is found to be described by the relation

$\rho_{\rm mag}(T < T_{\rm N}) = \rho(T < T_{\rm N}) - 3.85 \times 10^{-6}T^2 - 3.9 \times 10^{-4}\ \Omega$ cm $= 1.9 \times 10^{-6}T^4\ \Omega$ cm. The observations of both a T^4 term in $\rho_{\rm mag}(T < T_{\rm N})$ and a T^3 term in the specific heat is in accord with the observation of the AFM ordered state by the neutron diffraction measurements [2]. In addition the observed absence of an exponential dependence suggests the absence of an activated character (gapless activation) and thus weak anisotropic features.

The features of the resistivity isotherms can be classified into four different temperature regions (see figures 3 and 4). (i) For 15 K $< T <$ 300 K, the applied field (with Zeeman energy $< k_{\rm B}T$) reduces (very weakly) the resistive contributions from both CEF and spin fluctuation effects. (ii) For $T_{\rm N} < T <$ 15 K, $\rho(T, H)$ is, in contrast, strongly reduced since the magnetic field suppresses the contribution from both short-range effects and spin fluctuation. (iii) For $T_{\rm M} < T < T_{\rm N}$, an increase in the field induces a weak increase in $\rho(T, H)$ but, later above 4.2 T, it decreases at the same rate as that of, for example, 6 K; this indicates that, within $T_{\rm M} < T < T_{\rm N}$, the spins are not completely ordered. Finally, for the range (iv) $T < T_{\rm M}$, $\rho(T, H)$ increases strongly with H, reaching a maximum at $H_{\rm c}$ (the same value as the one shown in figure 1 and reported in the H–T phase diagram [3, 4]) and later decreases. Thus, it is evident that the dominant scattering mechanisms (other than the electron–phonon and defect interaction) are the spin fluctuation, CEF, and paramagnetic disorder at $T > T_{\rm M}$, while magnon scattering and spin fluctuation at $T < T_{\rm M}$.

An anomalous transition at $H_{\rm c}$ is evident in both the isothermal magnetization (figure 1) [3, 4] and $\rho(T < T_{\rm M}, H)$ (figure 4); in particular the peaks in the resistivity are symmetric about H. These observations, together with the inference that there is no ordering in the Co sublattice (see below), suggest that the event at $H_{\rm c}$ is *not* related to the (direct or indirect) itinerant metamagnetism of the Co sublattice. Rather, the event at $H_{\rm c}$ is most probably related to a field-induced rearrangement of the zero-field AFM order (possibly caused by a spin flip transition, or splitting of the lower CEF levels, etc). This is taken to be the reason behind the modification in the value of the component of the Ce moment along the field [3, 4] and the surge of additional resistive scattering as manifested in the peak feature of $\rho(T < T_{\rm M}, H)$. It is noticed that even at higher fields when the Ce spin is forced towards saturation (consequently $\rho(T < T_{\rm M}, H)$ towards lower values), the observed $\rho(T, 9\ {\rm T})$ (figure 4) is higher than $\rho(T, 0\ {\rm T})$ indicating that either the Ce saturated state has not been completely achieved or there is an additional field-dependent scattering from the Co subsystem.

A two-peak event is most evident in the zero-field specific heat (figure 2) as well as in the $\rho(T, 0\ {\rm T})$ curve (though manifested as two changes of slopes at 5.4(2) K and 4.7(1) K). Neighboring two magnetic events are not uncommon in the Ce-based ternary compounds; as examples, it is reported in Ce_3NiGe_2 [15] and in $CeNiGe_2$ [16]. It is unfortunate that the nature of this event in CeCoGe cannot be determined from the reported neutron diffractograms [2], since these were carried out only at 1.5 and 12 K. As neither CeNiGe [7] nor LaCoGe (see figure 2) are magnetically ordered, we considered that the surge of magnetic order in CeCoGe requires the simultaneous presence of the Co 3d and the Ce 4f subsystems. It can be argued that this two-peak event is due to the ordering of the Ce sublattice (occurring first at $T_{\rm N}$) which, at $T_{\rm M}$, is able to induce a strong local field that lead to the split of the Co 3d energy bands [17] (leading to a surge of Co itinerant moments and the eventual onset of their magnetic order). Though such features do occur as in the $Er_{1-x}Y_xCo_2$ system for example [18], in the present case, $T_{\rm M}$ transition cannot be related to a metamagnetic transition within the Co subsystem since the ordered Ce magnetic moment is too small: the zero-field value is 0.38(5) $\mu_{\rm B}$ [2], and reaches 1.34 $\mu_{\rm B}$ only at 14 T [2–4]. It is then safe to conclude that the $T_{\rm M}$ transition as well as the event at $H_{\rm c}$ are related to the rearrangement of the Ce moments. It is worth emphasizing that the contribution of the 3d subsystem to $N(E_{\rm F})$ (as reflected in the enhancement of γ) is important for the magnetic order in CeCoGe: the magnetic couplings in these ternary compounds are mediated by the indirect exchange coupling.

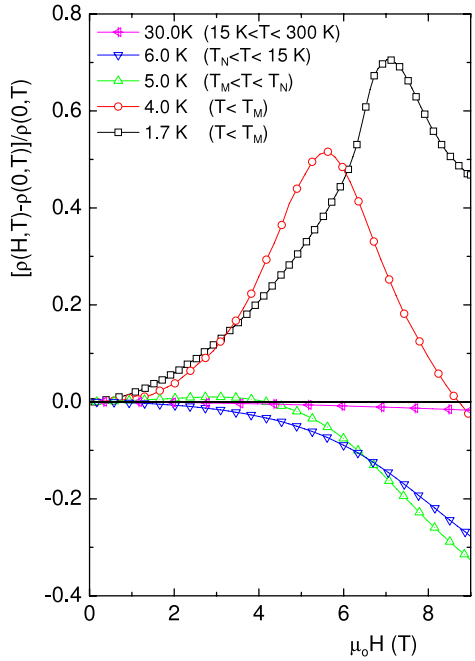

Figure 4. Field dependence of the normalized resistivity of CeCoGe $[\rho(T, H) - \rho(T, 0\ {\rm T})]/\rho(T, 0\ {\rm T})$.

4. Conclusion

It is evident that the low-temperature magnetic, thermal, and transport properties of CeCoGe are shaped by contributions from both the 4f and 3d subsystems. Based on a comparison with the ternary LaCoGe compound, we were able to identify the influence of each of the 4f and 3d electronic states on the studied low-temperature properties. On the one hand, the magnetic features of the Ce subsystem are observed in, as examples, the magnetic diffractograms of the ordered Ce sublattice, the magnetization isotherms (reflecting the Ce moment saturation), the magnetic specific heat contribution

(the collective motion of the 4f moments leading to a cubic-in-temperature term), and the resistivity below T_N (the electron–magnon scattering leading to a T^4-term). The contribution of the 3d subsystem, on the other hand, is manifested in the enhancement of $N(E_F)$ and in the thermal evolution of the resistivity (the quadratic term and the saturated features). Finally, both the field-induced transition at H_c (observed in the magnetization and resistivity isotherms) and the second peak at T_M (observed in the resistivity, magnetization, and specific heat) are attributed to a spin rearrangement of the AFM structure of the Ce sublattice.

Acknowledgments

We acknowledge partial financial support from the Czech Science Foundation (grant 202/06/0185) and the Brazilian agencies CNPq (485058/2006-5) and Faperj (E-26/171.343/2005).

References

[1] Welter R, Venturini G and Malaman B 1993 *J. Alloys Compounds* **201** 191
[2] Chevalier B and Malaman B 2004 *Solid State Commun.* **130** 711
[3] Vejpravova J, Prokleska J, Janousova B, Andreev A V and Sechovsky V 2006 *Physica* B **378–380** 797
[4] Andreev A V, Vejpravova J, Prokleska J and Sechovsky V 2008 *Physica* B **403** 744
[5] Chevalier B, Matar S, Marcos J S and Fernandez J R 2006 *Physica* B **378–380** 795
[6] Chevalier B, Matar S, Menetrier M, Marcos J S and Fernandez J R 2006 *J. Phys.: Condens. Matter* **18** 6045
[7] Kuang J P, Cui H J, Li J Y, Yang F M, Nakotte H, Bruck E and de Boer F R 1992 *J. Magn. Magn. Mater.* **104–107** 1475
[8] Kittel C 1963 *Quantum Theory of Solids* (New York: Wiley)
[9] Coqblin B 1977 *The Electronic Structure of Rare-Earth Metals and Aloys: the Magnetic Heavy Rare-Earth* (New York: Academic)
[10] Moriya T 1985 *Spin Fluctuation in Itinerant Electron Magnetism* (Berlin: Springer)
[11] Rossiter O L 1991 *The Electrical Resistivity of Metals and Alloys* (Cambridge: Cambridge University Press)
[12] Hauser R, Bauer E and Gratz E 1998 *Phys. Rev.* B **57** 2904
[13] Cornut B and Coqblin B 1972 *Phys. Rev.* B **5** 4541
[14] Kadowaki K and Woods S B 1986 *Solid State Commun.* **58** 507
[15] Durivault L, Bourgee F, Chevalier B, Isnard O, Andre G, Weill F and Etourneau J 2003 *Acta Phys. Pol.* B **34** 1393
[16] Jung M H, Lacerda A H, Pagliuso P G, Sarrao J L and Thompson J D 2002 *J. Appl. Phys.* **91** 8522
[17] Bloch D, Edwards D M, Shimizu M and Voiron J 1975 *J. Phys. F: Met. Phys.* **5** 1217
[18] Hauser R, Bauer E, Gratz E, Müller H, Rotter M, Michor H, Hilscher G, Markosyan A, Kamishima K and Goto T 2000 *Phys. Rev.* B **61** 1198